



Contents lists available at ScienceDirect

Global and Planetary Change

journal homepage: www.elsevier.com/locate/gloplacha

Late Quaternary stratigraphy and sedimentation patterns in the western Arctic Ocean

Leonid Polyak^{a,*}, Jens Bischof^b, Joseph D. Ortiz^c, Dennis A. Darby^b, James E.T. Channell^d, Chuang Xuan^d, Darrell S. Kaufman^e, Reidar Løvlie^f, David A. Schneider^g, Dennis D. Eberl^h, Ruth E. Adler^a, Edward A. Councilⁱ^a Byrd Polar Research Center, Ohio State University, Columbus, OH 43210, USA^b Department of Ocean, Earth, and Atmospheric Sciences, Old Dominion University, Norfolk, VA 23529, USA^c Department of Geology, Kent State University, Kent, OH 44242, USA^d Department of Geological Sciences, University of Florida, Gainesville, FL 32611, USA^e Department of Geology, Northern Arizona University, Flagstaff, AZ 86011, USA^f Department of Earth Science, University of Bergen, Norway^g IEEE Spectrum, 3 Park Avenue, New York, NY 10016, USA^h U.S. Geological Survey, Boulder, CO 80303, USAⁱ Department of Geological Sciences, Wright State University, Dayton, OH 45435, USA

ARTICLE INFO

Article history:

Accepted 17 March 2009

Available online xxx

Keywords:

Arctic Ocean
sediment stratigraphy
sedimentary environments
Late Quaternary
glaciations

ABSTRACT

Sediment cores from the western Arctic Ocean obtained on the 2005 HOTRAX and some earlier expeditions have been analyzed to develop a stratigraphic correlation from the Alaskan Chukchi margin to the Northwind and Mendeleev–Alpha ridges. The correlation was primarily based on terrigenous sediment composition that is not affected by diagenetic processes as strongly as the biogenic component, and paleomagnetic inclination records. Chronostratigraphic control was provided by ¹⁴C dating and amino-acid racemization ages, as well as correlation to earlier established Arctic Ocean stratigraphies. Distribution of sedimentary units across the western Arctic indicates that sedimentation rates decrease from tens of centimeters per kyr on the Alaskan margin to a few centimeters on the southern ends of Northwind and Mendeleev ridges and just a few millimeters on the ridges in the interior of the Amerasia basin. This sedimentation pattern suggests that Late Quaternary sediment transport and deposition, except for turbidites at the basin bottom, were generally controlled by ice concentration (and thus melt-out rate) and transportation distance from sources, with local variances related to subsurface currents. In the long term, most sediment was probably delivered to the core sites by icebergs during glacial periods, with a significant contribution from sea ice. During glacial maxima very fine-grained sediment was deposited with sedimentation rates greatly reduced away from the margins to a hiatus of several kyr duration as shown for the Last Glacial Maximum. This sedimentary environment was possibly related to a very solid ice cover and reduced melt-out over a large part of the western Arctic Ocean.

Published by Elsevier B.V.

1. Introduction

Despite its significance for the study of climate change and the potential for the search of new mineral resources, both the modern sedimentary regime and the history of sedimentation in the Arctic Ocean remain only fragmentarily understood. Even the stratigraphic framework for Arctic marine geological and paleoclimatic studies is far from being established. In particular, the western Arctic Ocean, covered by perennial ice and hydrographically isolated by a gyre circulation, is the least understood oceanic region on Earth both in terms of its long-term and recent geologic history. Meanwhile, this is the region experiencing probably the most dramatic change today, with sea-ice cover diminishing beyond any expectations (Comiso et al., 2008; Stroeve et al., 2008).

Investigation of the Quaternary stratigraphy and paleoceanography of the western Arctic was recently boosted by the results of the 2005 Healy–Oden TransArctic Expedition (HOTRAX) (Darby et al., 2005). Material collected on this transect included sediment cores raised from the major ridges and plateaus of the Arctic Ocean floor such as the Northwind, Mendeleev, Alpha, and Lomonosov ridges, and high-resolution cores from the Alaskan Chukchi margin (Fig. 1). We use the HOTRAX as well as some earlier collected cores to develop a stratigraphic correlation and outline the major patterns of sediment deposition from the Alaskan margin to the interior of the western Arctic Ocean. Analysis of this sedimentary archive is much needed for understanding the paleoclimatic evolution of the Arctic.

2. Geographic and stratigraphic context

The two roughly equal parts of the Arctic Ocean located in the Western and Eastern Hemispheres, and commonly termed the western and eastern Arctic, largely correspond to the Amerasia and Eurasia

* Corresponding author. Fax: +1 614 292 4697.

E-mail address: polyak.1@osu.edu (L. Polyak).

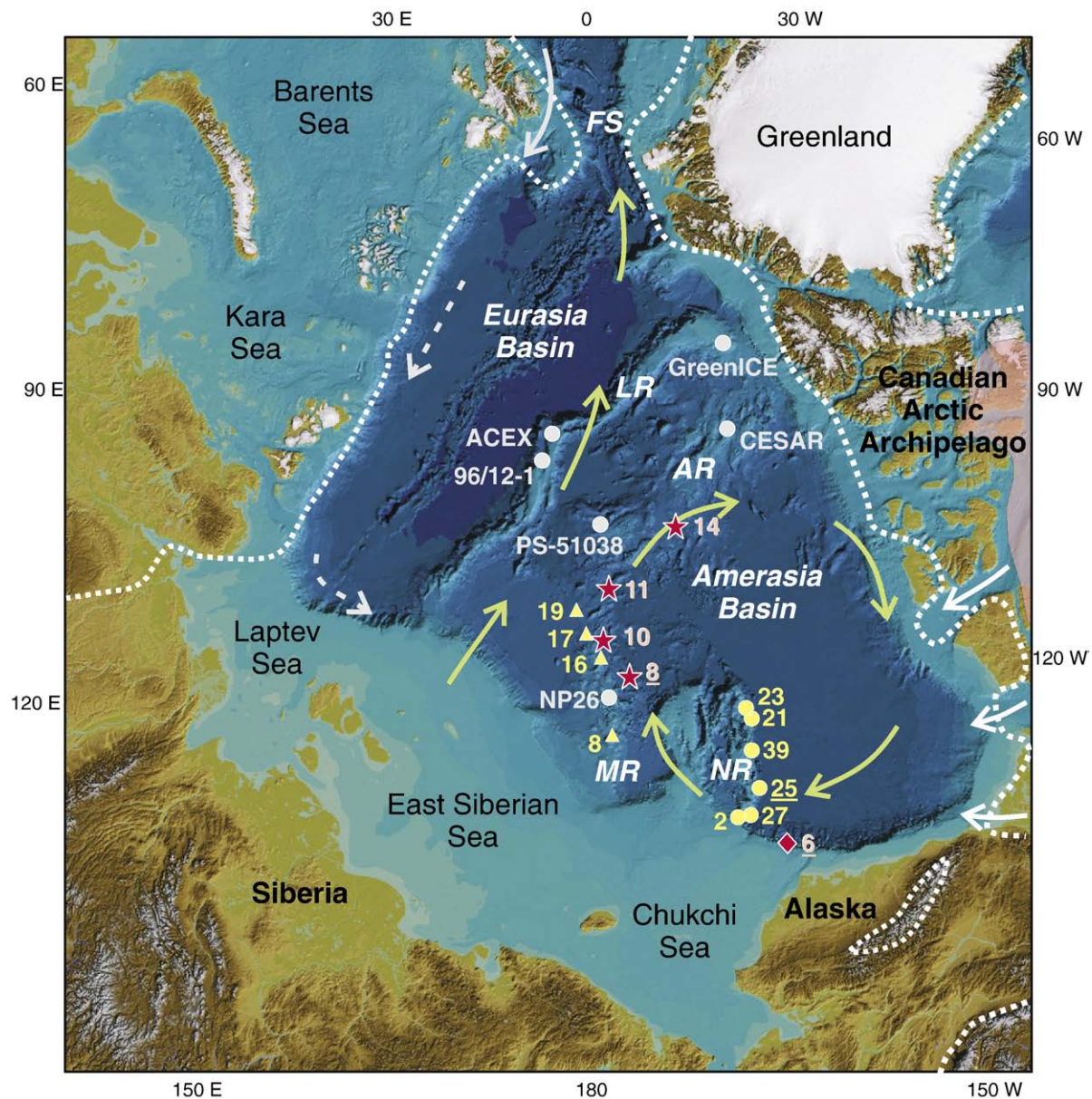


Fig. 1. Index map of the Arctic Ocean showing core sites used in the paper: red diamond/stars are HOTRAX cores HLY0501/03, yellow circles/triangles are P1-92/94-AR piston/box cores, grey circles are other published data. LR, MR, AR, and NR are Lomonosov, Mendeleev, Alpha, and Northwind ridges, respectively; FS—Fram Strait. Colored arrows show major circulation features: Beaufort Gyre, Transpolar Drift, and Atlantic-water inflow (dashed arrows for subsurface current). Base map is the International Bathymetric Chart of the Arctic Ocean (IBCAO-2; Jakobsson et al., 2008a). Dotted lines show the maximal limit of Late Pleistocene glaciations in North America and Eurasia (Dyke et al., 2002; Svendsen et al., 2004), and white arrows show major ice streams at the northern Laurentide margin (Stokes et al., 2005, 2006; Kleman and Glasser, 2007). Semitransparent pink fill in the Canadian Archipelago shows the major source area for dolomitic detrital carbonates in the western Arctic Ocean.

deep-sea basins separated by the Lomonosov Ridge. While the eastern Arctic has a considerable water exchange with the North Atlantic, the western Arctic is more isolated hydrographically due to the Beaufort Gyre surface circulation system and the Lomonosov Ridge barrier to deep water exchange. These conditions in the western Arctic Ocean account for a longer residence time of both surface and deep water masses, heavier ice coverage, high level of endemism in marine biota, and largely self-contained depositional system. This isolation complicates stratigraphic and paleoclimatic studies in the western Arctic by making it very difficult to compare the history of this region with other oceans. Combined with low sedimentation rates, strong dissolution of biogenic skeletal remnants, and logistical problems of obtaining sedimentary records from areas of interest, this setting explains the very slow progress and controversial results in developing the stratigraphy

and reconstructing paleoceanography of the western Arctic despite half a century of marine geological exploration.

The early sediment cores from the central Arctic Ocean, collected from Russian ice camps in the 1950s, were shown to hold a record of cyclic lithological and microfaunal variations interpreted to be linked with circum-Arctic glacial and sea-level changes (Belov and Lapina, 1961, 1970). This approach allowed for the first age estimate of Arctic Ocean sediments by importing the contemporaneous age model for Quaternary glaciations in northern Eurasia, which gave meaningful results. Ericson et al. (1964) used a similar approach relating lithological banding to climatic variations in sea-ice cover. Subsequent studies of the 1960s through 1980s, based on sediment cores raised from the western Arctic by the US ice camp T-3, relied on paleomagnetic inclination data to constrain the age model (e.g., Steuerwald

et al., 1968; Herman, 1969; Clark, 1970; Hunkins et al., 1971). These paleomagnetic data, generated on discrete samples commonly averaging over the core intervals of ca. 10 cm, showed a crude, but overall consistent pattern of changes in the inclination record. The intervals with consistently high or, alternatively, low inclination values were interpreted as paleomagnetic polarity chrons and correlated to the global polarity scale. In particular, the prominent drop in the inclination was found in the upper 0.5 to 1.5 m in practically all cores and interpreted as the Bruhnes–Matuyama boundary; similarly, other inferred changes in the polarity found downcore were interpreted as Matuyama–Gauss and Gauss–Gilbert boundaries. Ages for the entire sediment record were interpolated between these boundaries. Regardless of the age model, several lithostratigraphic units were traced across the western Arctic Ocean and interpreted in terms of paleoclimatic and sedimentary changes. Y. Herman (1969, 1974) identified three broad sedimentary and microfaunal units and interpreted them to represent three paleoclimatic regimes roughly corresponding to the inferred Bruhnes, Matuyama, and Gauss polarity chrons. The group led by D. Clark paid more attention to lithological details and identified several lithostratigraphic units, indexed A to M, that were successfully used for correlating cores across the western Arctic Ocean, both from T-3 and later collections (e.g., Clark et al., 1980; Jackson et al., 1985; Phillips and Grantz, 1997). A notable lithostratigraphic feature in these sediments is the presence of detrital carbonate layers, which have a similar clast petrography, with high dolomite contents, and can be correlated across the entire western Arctic Ocean. These layers represent the pulsed dispersal of eroded bedrock carbonates from the Canadian Arctic by Laurentide icebergs and can be used as event-stratigraphy markers similar to Heinrich events in the North Atlantic (Darby, 1971; Bischof et al., 1996; Phillips and Grantz, 2001).

Despite the significant progress in understanding sedimentary processes and paleoclimatic environments achieved in the works of D. Clark, Y. Herman and other investigators of the 1960s through 1990s, the stratigraphy based on a simplistic reading of the inclination data started to display apparent shortcomings such as discrepancies of derived sedimentation rates with AMS ^{14}C ages (Darby et al., 1997) and geophysical records (Backman et al., 2004), as well as problems with reconciling the age model with the history of Arctic glaciations and sea-level change (Polyak et al., 2004). The latter factor had a profound impact on the Arctic Ocean, which shrunk by 1/3 of its area, was bordered by continental ice sheets along at least half of its perimeter, and had a very restricted connection with other oceans during glacial periods. Meanwhile, the polarity-based age model and very low derived sedimentation rates resulted in inconsistent placement of glacial vs. interglacial intervals and often controversial paleoclimatic interpretations.

The new stratigraphic paradigm was introduced for a sedimentary record Oden 96/12-1PC from the central Lomonosov Ridge (Jakobsson et al., 2000). A detailed, 1-cm-step paleomagnetic record used in this

work indicated a more complex pattern of the inclination changes than in previous studies and was interpreted to reflect short-lived excursions of the magnetic field rather than long-term polarity changes. Furthermore, the cyclic color banding in the core, driven by the varying content of manganese oxides, was correlated to the global Marine Isotopic Stages (MIS) based on the inference that brown, Mn-rich layers correspond to interglacial/interstadial periods. This was essentially a repetition of the approach suggested 40 years earlier (Belov and Lapina, 1961, 1970), but now strengthened with an up-to-date Quaternary time scale. The new paleomagnetic and cyclostratigraphic approach gave consistent results, further corroborated by the coccolith data in 96/12-1PC (Jakobsson et al., 2001; Backman et al., 2004). The resulting stratigraphy provided a more realistic assessment of sedimentation rates and placement of paleoclimatic events than in earlier studies.

Regardless of the interpretation of the Arctic Ocean paleomagnetic inclination record, its consistent juxtaposition with independent lithological, paleontological, and chronostratigraphic features allowed for the expansion of the new age model to other cores from the Lomonosov Ridge and some other sites across the Arctic Ocean with comparable sedimentation rates (Backman et al., 2004; Polyak et al., 2004; Spielhagen et al., 2004; Kaufman et al., 2008). Recently this age model has been also shown to be consistent with longer-term Cenozoic stratigraphy developed for the first deep-drilling record from the central Arctic (ACEX; O'Regan et al., 2008). However, correlation between distant areas with different sedimentation regimes is not straightforward (e.g., Sellén et al., 2008), and some basic questions such as the origin of the inclination swings still pertain to the Arctic Ocean stratigraphy.

One way to improve the stratigraphy is to correlate the deep-sea records to those from surrounding continental margins, which offer much higher sedimentation rates. However, developing such correlation faces many difficulties as the Quaternary record preceding the last deglaciation is typically eroded on shallow and/or glaciated shelves, carbonate dissolution is strong near the margins, and facies changes complicate the comparison of litho- and biostratigraphies. In this paper we capitalize on the HOTRAX cores from the Alaskan Chukchi margin, from the shelf to mid-slope, to establish a step-wise correlation of these records with the proximal (Northwind Ridge) and more distal (Mendelev and Alpha Ridges) deep-sea areas of the western Arctic Ocean. The Holocene stratigraphy of the Alaskan margin cores is elaborated in a series of recent and concurrent papers (Darby et al., 2001; Andrews and Dunhill, 2004; De Vernal et al., 2005; Keigwin et al., 2006; Barletta et al., 2008; McKay et al., 2008; Darby et al., in press; Lisé-Pronovost et al., in press). We investigate the pre-Holocene record recovered in cores from the slope and compare it with cores from the Northwind and Mendelev ridges. Because of only patchy preservation of biological proxies in Arctic sediments, especially at the margins, in this work we primarily use mineralogical

Table 1
Sediment cores investigated for this study.

| Core ID | Latitude N | Longitude W | Water depth (m) | Piston core length (cm) | Area |
|---------------|---------------|----------------|--------------------|----------------------------|-----------------|
| HLY0501-6JPC* | 72° 30.7' | 157° 02.1' | 673 | 1554 | Alaskan margin |
| HLY0503-8JPC* | 79° 35.6' | 172° 30.1' | 2792 | 1188 | Mendelev Ridge |
| HLY0503-10JPC | 81° 13.6' | 177° 11.6' | 1865 | 1272 | Mendelev Ridge |
| HLY0503-11JPC | 83° 08.6' | 174° 32.2' | 2644 | 1019 | Mendelev Ridge |
| HLY0503-14JPC | 84° 18.2' | 149° 02.0' | 1856 | 1133 | Alpha Ridge |
| P1-92AR-P2 | 73° 57.3' | 161° 31.7' | 369 | 348 | Northwind Ridge |
| P1-92AR-P25* | 74° 49.1' | 157° 21.9' | 1625 | 562.5 | Northwind Ridge |
| P1-92AR-P27 | 74° 00' | 157° 36.5' | 1214 | 753 | Northwind Ridge |
| P1-92AR-P39 | 75° 50.7' | 156° 01.9' | 1470 | 687 | Northwind Ridge |
| P1-93AR-P21 | 76° 51.8' | 154° 12.9' | 1470 | 683 | Northwind Ridge |
| P1-93AR-P23 | 76° 57.3' | 155° 03.9' | 951 | 572 | Northwind Ridge |

Asterisks indicate cores studied in most detail.

sediment characteristics along the lines explored in some earlier studies of the Chukchi margin (Darby et al., 2001; Polyak et al., 2007), combined with paleomagnetic stratigraphy and ^{14}C and amino-acid ages.

3. Materials and methods

In this study we use sediment cores collected on the HOTRAX'05 expedition (USCGC Healy 2005; HLY0501 and HLY0503) (Darby et al., 2005) and the US Geological Survey core collections from 1992–1994 (P1-92/94-AR) (Scientific Party, 1993; Aagard et al., 1996) (Table 1; Fig. 1). We choose cores from submarine ridges to avoid turbidite deposits that are common in deeper basins (e.g., Clark et al., 1980; Backman et al., 2004). To assemble the composite stratigraphy extending from the Alaskan continental margin into the deep western Arctic Ocean, we use a number of independent proxies for developing correlation between the selected cores and constraining the ages of the developed stratigraphy (Figs. 2–4).

Because of the widespread dissolution of biogenic calcite in sediments from the Alaskan margin and some stratigraphic intervals further offshore, foraminifers cannot be used for detailed correlation in these areas. To bridge the Alaskan margin and the adjacent deep-sea stratigraphy we use mineral, predominantly terrigenous components that are unlikely to be affected by diagenetic processes. The applicability of this approach has been demonstrated for the deglacial and Holocene sediments in the area where the Northwind Ridge branches off the Chukchi margin (Polyak et al., 2007). To obtain the most useful information on sediment composition for correlation between the Alaskan margin and the Northwind Ridge (Fig. 2), we used coarse-grain size, identification of clasts $>250\ \mu\text{m}$, mineralogy of detrital iron

oxide grains, quantitative X-ray diffraction, and/or X-ray fluorescence determination of chemical composition of bulk sediment. Composition of clasts $>250\ \mu\text{m}$ and iron oxide grains in the 45–250 μm fraction were analyzed in cores HLY0501-6JPC and P1-92AR-P25 (Fig. 2); results were matched to a circum-Arctic source database to determine sources of sediment delivered by icebergs and/or sea ice (Darby and Bischof, 1996; Darby, 2003). The quantitative XRD was performed on bulk sediment excluding grains $>250\ \mu\text{m}$ from core HLY0501-6JPC (Fig. 2) using the RockJock program for computing composition of minerals that were selected based on expected mineralogy and inspection of the XRD patterns (Eberl, 2003, 2004 for analytical detail). XRF was measured using an energy-dispersive Innov-X Alpha series handheld analyzer on whole HOTRAX cores at increments between 2 and 6 cm and on discrete samples in P1-92AR-P25. This analyzer with a 14-mm-wide integration window can measure up to 29 elements with detection limits in the range of 10–100 ppm depending on the element. Replicate measurements performed indicate 2-sigma errors between 2 and 10%. Overall, results for major and some of the minor elements is comparable with the Itrax XRF determinations on Arctic sediments from the Lomonosov Ridge (e.g., Löwemark et al., 2008). Correlation between the deep-sea cores, from the Northwind to Mendeleev and Alpha ridges, was based on XRF composition, foraminiferal abundance, and paleomagnetic inclination data (Figs. 2 and 4). Natural remanent magnetization (NRM) in HOTRAX cores HLY0503-8JPC, 10JPC, and 11JPC (Fig. 4a) was measured at the University of Florida. U-channel samples were measured at 1-cm spacing after alternating field (AF) demagnetization at 14 steps in the 10–100 mT peak-field range. Component magnetization directions were determined using the standard principal component analysis (Kirschvink, 1980). Core HLY0503-14JPC was analyzed using similar

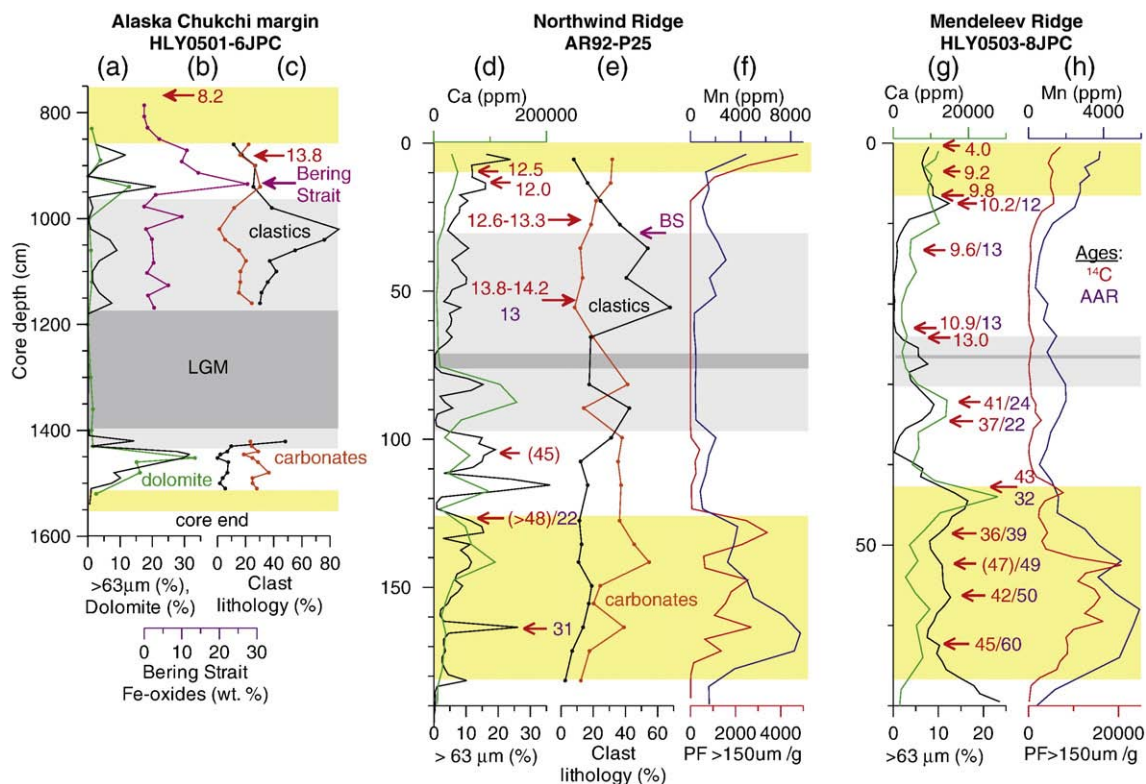


Fig. 2. Correlation of sediment cores from the Alaskan margin to the Mendeleev Ridge: sand content ($>63\ \mu\text{m}$) (a, d, g—black), XRD dolomite content (a—green), Bering Strait Fe-oxide matches spliced from HLY0501-5JPC (b—magenta), carbonate and clastic sedimentary IRD $>250\ \mu\text{m}$ (c and e—orange and black, respectively), XRF Ca content (d and g—green), XRF Mn content (f and h—blue), planktonic foraminifers $>150\ \mu\text{m}$ (f and h—red). ^{14}C and AAR ages (ka)—in red and purple, respectively; ^{14}C ages outside the calibration limit are shown in parentheses. Ages between 20–60 cm (arrows pointing to the right) and Bering Strait Fe-oxide peak (BS) for 92AR-P25 are spliced from 92AR-P2 (Polyak et al., 2007). Yellow shading—interglacial/interstadial units, light gray—interval with clastic IRD, dark gray—fine-grained LGM sediment. Note a large difference in core depth scales.

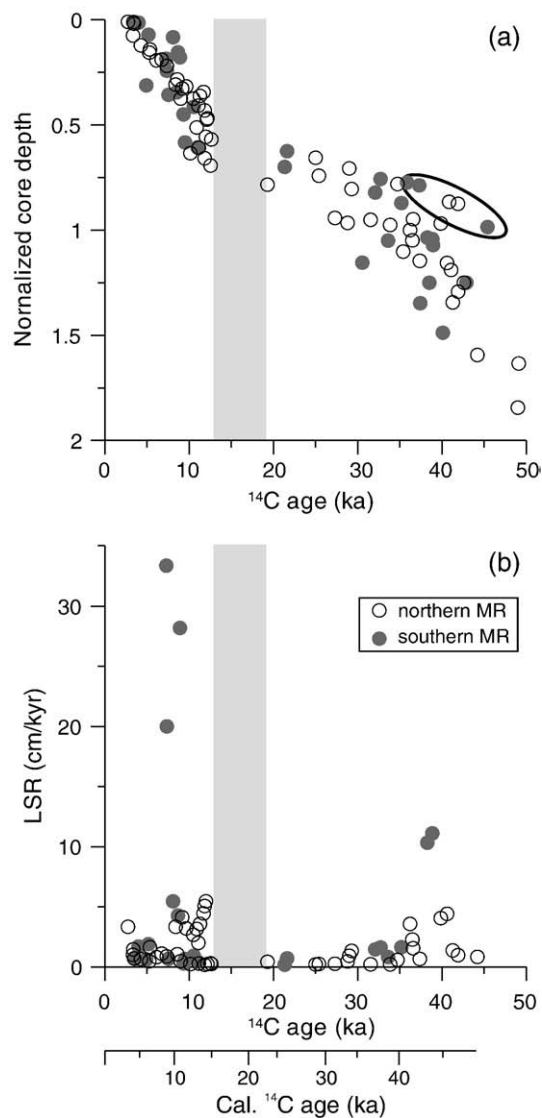


Fig. 3. Distribution of ^{14}C ages vs. core depth (a) and linear sedimentation rates (LSR) (b) in cores from the Mendeleev Ridge (northern and southern MR data shown by different symbols). ^{14}C data are from Darby et al. (1997), Poore et al. (1999a), Polyak et al. (2004), and Kaufman et al. (2008). Only standard oceanic reservoir correction is applied to ^{14}C ages. Calibrated age scale is shown below. Core depth is normalized to the top of the second brown unit. Grey shading shows the LGM hiatus. Old ages around the interval of high detrital carbonate content are enclosed by an oval. The LSR value of 33 cm/kyr at ca. 8 ka is not shown.

NRM measurement methods at 2-cm interval (measurements with a 2G pass-thru-magnetometer at Laboratoire des Sciences du Climat et de l'Environnement, Gif-sur-Yvette, and data-analysis at the University of Bergen). NRM measurements on P1-92/93-AR cores (Fig. 4b) were done by D. Schneider at the paleomagnetic laboratory of University of Rhode Island on discrete 2-cm-wide samples (increments between 5 and 15 cm) at demagnetization treatment levels between 0 and 80 mT.

Accelerator Mass Spectrometry (AMS) ^{14}C ages were measured on non pretreated planktonic (benthic in HLY0501-6JPC) foraminiferal samples of 5–8 mg from abundance maxima in several cores at the Arizona AMS Lab. Planktonic foraminifers (*Neogloboquadrina pachyderma* sin) from most of the same intervals and abundance maxima further downcore were analyzed for amino-acid racemization (AAR) with a focus on aspartic and glutamic acids (Kaufman et al., 2008). Each sample was analyzed in two to nine subsamples (average = 5), each composed of 3 to 10 Nps tests (average = 8). AAR-based ages

were calculated using the calibration developed by Kaufman et al. (2008) based on 47 samples from the Arctic Ocean whose ages were determined independently based on ^{14}C and correlations with the global marine oxygen isotope record; the AAR age uncertainties were estimated as about 15% at $\pm 2\sigma$ intra-sample variability. The calibration base included 30 samples whose AAR ages are presented in this study. Although ^{14}C age determination is more accurate than the AAR approach, the latter can be used for a longer time interval, estimated to ca. 150 ka in the Arctic Ocean (Kaufman et al., 2008), and is not affected by differences in reservoir ages. The combination of both dating methods is desirable for a comprehensive age assessment. New ^{14}C and AAR ages used in Figs. 2 and 4 are listed in Tables 2 and 3 except for ages from HLY0503-8JPC and HLY0501-6JPC, which are reported in Kaufman et al. (2008), and Lisé-Pronovost et al. (in press).

4. Results

4.1. Correlation between the Alaskan margin and deep-sea cores

Core HLY0501-6JPC features the longest continuous stratigraphic record among cores from the Alaskan Chukchi margin and was therefore chosen to exemplify sediment stratigraphy of this area (Fig. 2). The upper sedimentary unit in these cores reaches more than 10-m thickness and consists of fine-grained, bioturbated sediment with numerous reduced organic remains turned into black iron sulfides. This sediment represents the Holocene environment generally similar to modern, with variable, seasonal ice cover, relatively high biological productivity, and high sediment fluxes from the shelf (De Vernal et al., 2005; Darby et al., in press; McKay et al., 2008; Ortiz et al., in press). Multiple ^{14}C dates and paleomagnetic age markers consistently constrain the basal age of this unit to ca. 8.5 ka and average sedimentation rates to over 1 m/kyr (Barletta et al., 2008; Lisé-Pronovost et al., in press; McKay et al., 2008). The underlying sediment (below 855 cm in HLY0501-6JPC) is much more heterogeneous and contains laminations of various thicknesses and distinctness and variable numbers of coarse, ice-rafted debris (IRD) of mm- to cm-scale sizes. This type of sediment is characteristic of proglacial marine environments with strongly changeable sediment inputs from the glacial margin and extensive sediment dispersal by icebergs (e.g., Syvitski, 1991). A prominent fine-grained, mostly IRD-free interval is identified within the glaciomarine unit, between 11.8 and 14 m in HLY0501-6JPC (Fig. 2). Below 15 m this core reached sediment with patches of iron sulfides resembling the Holocene unit, but with some coarse IRD (Fig. 2).

To develop a correlation of the high-resolution record from the Alaskan margin, represented by HLY0501-6JPC, to the deep-sea areas of the western Arctic Ocean, we used cores P1-92AR-P25 and HLY0503-8JPC from the Northwind and Mendeleev Ridges, respectively (Fig. 2). These cores were selected based on relatively expanded thickness of stratigraphic units, and thus elevated sedimentation rates, in the upper part of the stratigraphy (see Adler et al., in press, for detail on core HLY0503-8JPC). A strong gradient in both sediment fluxes and biological production from the margin to the interior of the Arctic Ocean (e.g., De Vernal et al., 2005), results in differing thickness and appearance of sedimentary units. For example, reductive, olive-gray Holocene mud with numerous black iron-sulfide patches on the margin is replaced by a thin, brown mud unit in the deep sea, with similar units characterizing earlier interglacial/interstadial intervals (Jakobsson et al., 2000; Polyak et al., 2004). The brown color in this sediment is controlled by manganese hydroxides, which formation and/or preservation is enhanced by oxidative environment due to efficient bottom-water ventilation, slow sediment accumulation, and low content of labile organic matter (e.g., Stein et al., 2004). Despite these apparent differences between the margin and the central Arctic, distribution of various proxies in records under study shows a lot of similarity (Fig. 2).

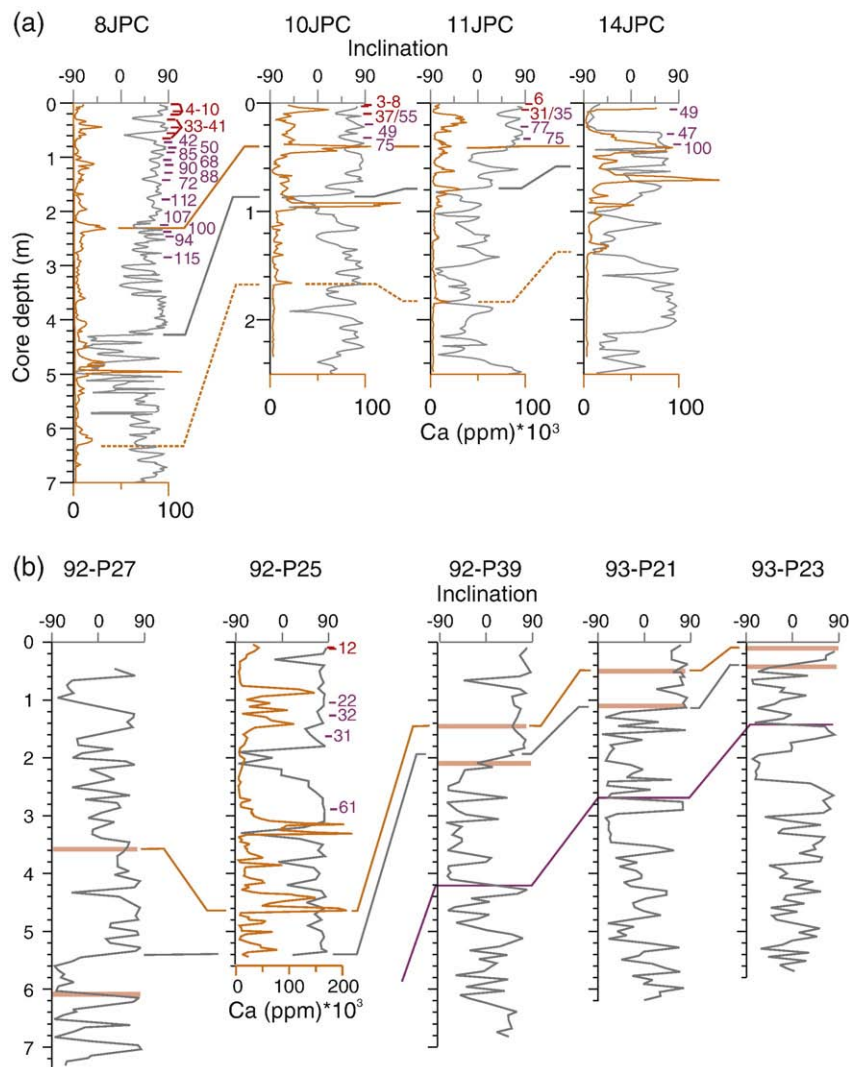


Fig. 4. Correlation of paleomagnetic inclination and detrital carbonates (XRF Ca content) for upper parts of HOTRAX cores from Mendeleev-Alpha ridges (a) and P1-92/93-AR cores from the Northwind Ridge (b), south to north (Fig. 1 for core location). Where Ca content not measured, carbonate layers are shown by pink bars based on core descriptions. Correlation lines are shown for a prominent carbonate layer at ca. MIS 5/6 boundary (orange), inclination drop (grey), base of detrital carbonate deposition (punctured orange, panel (a) only), and top of brown sediment (purple, panel (b) only). ^{14}C and AAR ages (ka) are shown in red and purple, respectively. ^{14}C ages in core HLY0503-8JPC are grouped; see Fig. 2 for details of the upper part of this core and P1-92AR-P25. Note a two-fold change in core depth scale between southern and northern Mendeleev Ridge cores (between 8JPC and 10JPC).

The two groups of IRD clasts, detrital carbonates and clastic sedimentary fragments, have been shown useful for reconstructing the history of iceberg-controlled sedimentation on the Chukchi margin

during the last deglaciation (Polyak et al., 2007). The consistent downcore distribution pattern of these IRD types in HLY0501-6JPC and P1-92AR-P25 (Fig. 2) as well as in cores analyzed earlier from the

Table 2
Radiocarbon ages of planktonic foraminifers.

| Lab ID ^a | Core ID | Depth in core (cm) | ^{14}C age (yr BP) | 1 σ (\pm) | Calibrated age (yr BP) ^b | 1 σ range (\pm) |
|---------------------|-------------|--------------------|-----------------------------|----------------------|-------------------------------------|----------------------------|
| UCIAMS 53933 | 8JPC | 3–4 | 8530 | 25 | 9167 | 58 |
| UCIAMS 53934 | 8JPC | 25–26 | 11,445 | 30 | 12,953 | 42 |
| AA75844 | 10MC2 | 0–0.5 | 3744 | 38 | 3673 | 68 |
| AA80408 | 10MC2 | 0.5–2 | 7135 | 55 | 7608 | 49 |
| AA75845 | 10MC2 | 10–11 | 31,760 | 430 | 36,731 | 457 |
| AA75846 | 11MC2 | 0–0.5 | 6065 | 51 | 6488 | 68 |
| AA75847 | 11MC2 | 5–6 | 26,140 | 220 | 30,949 | 270 |
| AA74468 | P1-92AR-P2 | 136–137.5 | 12,783 | 58 | 14,226 | 126 |
| UCIAMS 53935 | P1-92AR-P25 | 9–10.5 | 10,940 | 30 | 12,522 | 43 |
| AA75848 | P1-92AR-P25 | 13–14 | 10,639 | 52 | 11,962 | 68 |
| AA75849 | P1-92AR-P25 | 105–106 | 45,200 | 2200 | na | na |
| AA75850 | P1-92AR-P25 | 127–128 | >47,800 | na | na | na |

^a Samples were analyzed by AMS at the NSF Radiocarbon Facility, University of Arizona (AA) or University of California, Irvine (UCIAMS).

^b Holocene ages are median probability ages based on calibration using CALIB v 5.0.2 (<http://calib.qub.ac.uk/calib>); older ages were calibrated using the Fairbanks0107 program (Fairbanks et al., 2005). No ΔR was applied.

Table 3
Extent of amino-acid racemization (D/L) in planktonic foraminifers.

| Lab ID (UAL) | Core ID | Depth in core (cm) | n^a | | Aspartic acid | | Glutamic acid | | Age (ka) ^b |
|-----------------|----------------|-----------------------|-------|---|---------------|----------------|---------------|----------------|--------------------------|
| | | | | | D/L | $\pm \sigma_x$ | D/L | $\pm \sigma_x$ | |
| 5924 | P1-92AR-P2 | 136–137.5 | 4 | 0 | 0.093 | 0/006 | 0.051 | 0.016 | 13 |
| 6145 | P1-92AR-P25 | 105–106 | 7 | 0 | 0.195 | 0.009 | 0.075 | 0.007 | 22 |
| 6508 | P1-92AR-P25 | 127–128 | 6 | 1 | 0.242 | 0.009 | 0.096 | 0.007 | 32 |
| 6146 | P1-92AR-P25 | 163–164 | 6 | 1 | 0.232 | 0.015 | 0.098 | 0.007 | 31 |
| 6509 | P1-92AR-P25 | 289 | 2 | 3 | 0.315 | 0.028 | 0.140 | 0.033 | 61 |
| 6511 | HLY0503-10MC-2 | 10–11 | 5 | 0 | 0.279 | 0.009 | 0.137 | 0.005 | 55 |
| 6875 | HLY0503-11MC-2 | 20–21 | 6 | 2 | 0.274 | 0.009 | 0.125 | 0.009 | 49 |
| 6876 | HLY0503-11MC-2 | 34–35 | 6 | 3 | 0.338 | 0.007 | 0.156 | 0.011 | 75 |
| 6510 | HLY0503-11MC-2 | 5–6 | 5 | 0 | 0.225 | 0.018 | 0.106 | 0.011 | 35 |
| 6877 | HLY0503-11MC-2 | 23–24 | 8 | 1 | 0.333 | 0.006 | 0.163 | 0.008 | 77 |
| 6878 | HLY0503-11MC-2 | 33–34 | 6 | 1 | 0.337 | 0.013 | 0.156 | 0.015 | 75 |
| 6879 | HLY0503-14MC-5 | 6–7 | 8 | 1 | 0.268 | 0.008 | 0.126 | 0.008 | 49 |
| 6880 | HLY0503-14JPC | 29–30 | 5 | 3 | 0.261 | 0.007 | 0.125 | 0.005 | 47 |
| 6881 | HLY0503-14JPC | 39–40 | 5 | 2 | 0.373 | 0.008 | 0.193 | 0.005 | 100 |

^a n —Number of subsamples included; ex —number excluded in calculation of mean and standard error.

^b Age equation $t = (920(D/L_{Asp})^{2.3} + 1462(D/L_{Glu})^{1.6})/2$ (Kaufman et al., 2008).

southern Northwind Ridge (Polyak et al., 2007) confirms the region-wide character of sedimentation changes indicated by these proxies and their applicability for stratigraphic correlation. Clasts of weakly consolidated, mostly dark gray sedimentary rocks and coal have elevated content immediately above and below the prominent fine-grained interval, whereas carbonates predominate IRD in the rest of pre-Holocene stratigraphy in these cores. To enhance the characterization of detrital carbonate distribution, we used quantitative XRD data on selected samples from HLY0501-6JPC (Fig. 2). Results demonstrate that carbonates are predominantly composed of dolomite (up to 1/3 of bulk sediment) that is indicative of Lower Paleozoic strata in the Canadian Arctic (Fig. 1), which have been repeatedly eroded by the Laurentide ice sheets (e.g., Bischof et al., 1996; Phillips and Grantz, 2001; Vogt, 1997). The bulk of this dolomite in carbonate layers from the deep-sea cores is in the fine fractions, typical of rock flour from glacial scouring; whereas, in HLY0501-6JPC dolomite content corresponds to coarse IRD numbers, thus indicating a strong dilution of fine fractions by other depositional processes.

Correlation between western Arctic cores away from the continental margin can be achieved using more proxies such as foraminiferal numbers and Mn content, which is reflected in sediment color (Polyak et al., 2004; Kaufman et al., 2008; Adler et al., in press). Consistent downcore patterns in these proxies with high values in interglacial/interstadial units and lows in the intermittent glacial units are well expressed in both P1-92AR-P25 and HLY0503-8JPC (Fig. 2). The carbonate layers can also be clearly traced using the bulk Ca content (XRF measurements), which primarily represents detrital carbonates, whereas foraminiferal contribution is relatively negligible (Fig. 2). We have not performed coarse-grain identification in HLY0503-8JPC, but data on nearby NP26 cores (Polyak et al., 2004) indicate elevated numbers of sedimentary clasts in the same stratigraphic position as in P1-92AR-P25.

4.2. Age constraints for the last glacial (stadial) cycle

The use of ^{14}C stratigraphy in the Arctic Ocean is complicated by several factors. No pre-bomb material has been identified for the determination of apparent ages, as has been done on the Arctic margins (Mangerud and Gulliksen, 1975; McNeely et al., 2006), so we can only speculate regarding the reservoir ages of water masses in the central Arctic Ocean. The modern ages of the surface and halocline waters, the main habitats of adult arctic planktonic foraminifers that constitute the preferred material for ^{14}C dating, are on the order of just ten years (Ekwurzel et al., 2001), and we assume similar high ventilation rates for interglacial/interstadial periods characterized by high foraminiferal $\delta^{13}\text{C}$ (Polyak et al., 2004; Spielhagen et al., 2004). Nevertheless, ^{14}C ages from core tops consistently give ages as old as 1.5 to 3.5 ka (Darby et al., 1997; Poore et al., 1999a), which can be ex-

plained by either very low sedimentation rates in the late Holocene or anomalously high reservoir ages. Slow sediment accumulation combined with bioturbation provide a reasonable explanation for the observed ages, which is consistent with low sedimentation rates determined in the mid- to late Holocene in cores with relatively detailed age control (Darby et al., 1997; Poore et al., 1999a; Adler et al., in press). However, there is also a potential for anomalous reservoir ages or pre-formed ^{14}C concentrations in some areas and/or stratigraphic intervals. One possibility is that ages may be affected by the consumption of old, but partially labile organic matter with ages of nearly 2 kyr, that could be advected into the central Arctic Ocean from its margins (Hwang et al., 2008). Additionally, pulses of detrital carbonates dispersed with the Laurentide icebergs can bias ^{14}C composition in foraminiferal tests from respective layers through their contamination with fine-grained carbonate and/or through the accompanying release of hard water containing dissolved old carbonate (e.g., Heier-Nielsen et al., 1995). The latter factor may have been significant in the western Arctic as ^{14}C ages appear to be especially old on the Northwind Ridge, which is located closer to the Laurentide margin than the Mendeleev Ridge, as indicated by the comparison of ^{14}C and AAR ages in deglacial and pre-LGM sediments (Fig. 2). Because of these uncertainties, we treat all ^{14}C ages from pre-Holocene sediments as potentially biased towards older values.

Because of very scarce biogenic material in pre-Holocene sediments, only one such ^{14}C age was obtained in HLY0501-6JPC. Despite the uncertainties with age calibration, ages from this core and the correlative stratigraphies from the southern Northwind Ridge consistently indicate that sediments immediately above the prominent fine-grained interval (above 11.8 m in HLY0501-6JPC) were deposited during the last deglaciation (Fig. 2). This inference is corroborated by the spike in Fe-oxide grains from the Bering Strait source area identified in an adjacent core HLY0501-5JPC at the level correlated to ca. 930 cm in HLY0501-6JPC (see Barletta et al., 2008, and Lisé-Pronovost et al., in press, for stratigraphic details of cores HLY0501-5JPC and 6JPC, respectively). A similar spike has been interpreted in core P1-92AR-P2 from the southern end of the Northwind Ridge as a proxy for the re-opening of the Bering Strait during the sea-level rise around 12 ka (Polyak et al., 2007). Furthermore, the fine-grained interval in 92AR-P2 is underlain by a subglacial diamicton that had to be emplaced by the extension of the Laurentide ice sheet during the Last Glacial Maximum (LGM) (Polyak et al., 2007). This indicates that the fine-grained sediment was deposited during or immediately after the LGM, whereas the underlying interval with numerous IRD and reddish-brown goethite aggregates in HLY0501-6JPC (Grygar et al., 2007) represents the LGM advance of the northwestern Laurentide margin. In this case, sediment with iron sulfides in the bottom 15 cm of HLY0501-6JPC likely corresponds to the preceding interstadial. This inference is

corroborated by ^{14}C and AAR ages in the correlative stratigraphies on the Northwind and Mendeleev Ridges, which provide a crude but consistent chronostratigraphic picture including a prominent pre-LGM interstadial (Figs. 2 and 3). Based on this stratigraphy, the basal age of HLY0501-6JPC can be crudely estimated around 30 ka and average sedimentation rates of 30 cm/kyr for pre-Holocene sediments, or ca. 50 cm/kyr for the entire core. Sedimentation rates can be even higher at some sites along the Alaskan Chukchi margin due to local current and/or bathymetry controls on deposition (Barletta et al., 2008; Lisé-Pronovost et al., in press; Darby et al., in press).

A relatively detailed age control can be established for the upper part of the Quaternary stratigraphy on the Mendeleev Ridge where multiple ^{14}C ages have been generated on several sediment cores including HLY0503-8JPC and five cores investigated earlier (Fig. 3) (Darby et al., 1997; Poore et al., 1999a; Polyak et al., 2004; Kaufman et al., 2008; Adler et al., in press). Because differences in sedimentation rates between the sites complicate the comparison of age-depth distributions, for plotting purposes we have normalized the sample depths to the presumably synchronous level, the top of the second conspicuous brown unit representing the last major interstadial (e.g., 42 cm in HLY0503-8JPC). The ages in this unit extend to ca. 45–50 ka near its base, which matches the termination age of the penultimate glaciation in northern Eurasia (Svendsen et al., 2004; Larsen et al., 2006).

The resulting age-depth distribution shows a consistent, orderly pattern with a few reversals, mostly limited to the interval on top of the second brown unit, which features a high content of detrital carbonates (Figs. 2 and 3). The downcore age-depth pattern indicates a sedimentation rate increase towards the lower Holocene and the deglaciation (ca. 8–15 ka), then a conspicuous hiatus between ca. 15 and 23 ka, and another interval of scattered, but generally increasing sedimentation rates towards ca. 40 ^{14}C ka (Fig. 3). Linear sedimentation rates estimated between the ages in each core (excluding the reversals)¹ indicate that rates increase from top to the bottom of the Holocene mostly from around 1 cm/kyr to 5 cm/kyr, with extreme values as high as between 20 and 35 cm/kyr occurring around ca. 8–10 ka. A similar pattern is observed in the pre-LGM period where sedimentation rates increase to values exceeding 10 cm/kyr between ca. 35 and 40 ka. We believe that these abnormally high rates are real because they occur in two separate cores at the same stratigraphic intervals. We note that sedimentation rates are unevenly distributed between the sites, with an overall decrease away from the continental margin. The extremely high values above 10 cm/kyr are found only in cores P1-94AR-B8 and HLY0503-8JPC from the southern part of the Mendeleev Ridge.

The pronounced drop in sedimentation rates, or even a hiatus, during the LGM appears to be a robust feature in cores not only from the Northwind and Mendeleev Ridges (Figs. 2 and 3), but also as far as the Amerasian flank of the Lomonosov Ridge (core P1-94AR-B28; Darby et al., 1997). AAR ages also indicate this hiatus in HLY0503-8JPC, despite their generally smoother distribution with depth than ^{14}C ages (Kaufman et al., 2008; Adler et al., in press). An earlier study of low-resolution cores from the northern Mendeleev Ridge suggested that the hiatus was related to sea-floor winnowing by contour currents (Poore et al., 1999b), but our data show that this interval corresponds to sediment fining with no evidence of lag deposits (Fig. 2), which is indicative of a reduced deposition rather than winnowing. We note that it is difficult to constrain the age of such an event accurately because of possible contamination of samples across the hiatus.

4.3. Longer-time correlation between deep-sea cores

While cores from the Alaskan margin do not penetrate deeper than the estimated last interstadial (between ca. 30 and 45 ka), cores from

the Arctic Ocean interior recover much longer stratigraphies. In this paper we do not aim to investigate the entire stratigraphic range recovered by these cores, but focus on the Late Quaternary to upper Middle Quaternary time period, which has been characterized by a number of proxies in several key cores (e.g., Jakobsson et al., 2000; Polyak et al., 2004; Spielhagen et al., 2004; Kaufman et al., 2008; Adler et al., in press). A prominent stratigraphic feature that can be used for correlation is the change in paleomagnetic inclination record from mostly high values in the upper part of the record to variable, often low (including negative) values below. Recent studies suggest that this inclination drop occurred during Marine Isotopic Stage (MIS) 7, between 200 and 250 ka (Jakobsson et al., 2000; Spielhagen et al., 2004; O'Regan et al., 2008). We are cautious about relating this change to a specific variation of the geomagnetic field as proposed in these papers. Nevertheless, the inclination drop has a consistent position relative to independent proxies such as sediment color and density changes, foraminiferal numbers, and detrital carbonate layers, which indicates its validity for stratigraphic correlation.

We use the inclination data for correlation of sediment cores along the Mendeleev–Alpha and Northwind ridges, along with ^{14}C and/or AAR ages, and the position of detrital carbonate layers identified by visual description in all cores and characterized quantitatively in cores measured for XRF (Fig. 4). Other proxies such as foraminiferal abundance and Mn-controlled color banding show the same correlation pattern (Fig. 2) (Kaufman et al., 2008; Adler et al., in press), but it gets more difficult to discern in cores from the interior of the Amerasia Basin where the stratigraphy is more compressed (e.g., HLY0503-10 to 14). The inclination drop is well identifiable in most cores used in this study, as well as in earlier investigated western Arctic cores with paleomagnetic control (Jackson et al., 1985; Poore et al., 1993; Spielhagen et al., 2004). In cores with a compressed stratigraphy, where alternative interpretations of the position of the major inclination drop are possible, correlation is guided by the use of multiple proxies. Despite a considerable scatter, which may not allow for an accurate age determination for sediments older than the LGM, ^{14}C and AAR ages show an overall consistent downcore distribution that is especially helpful for correlating cores with different sedimentation rates (Fig. 2a).

The major detrital carbonate layers are clearly visible, especially in cores from the Northwind Ridge where they often constitute several centimeters in thickness (e.g., Poore et al., 1994; Phillips and Grantz, 1997, 2001). Further away from the Laurentide margin these layers may look more subtle, depending on background sedimentation rates and prevailing iceberg pathways, but they are easily identifiable from Ca content (e.g., Fig. 4). Ca distribution shows several distinct spikes and the level further downcore at which carbonates taper off. Two prominent carbonate layers that have highest Ca concentrations in most cores (e.g., around 230 and 500 cm in HLY0503-8; Fig. 4) have been long used for lithostratigraphic correlation as PW (pink-white) layers 2 and 1, at the bottom of Clark's units M and J (e.g., Clark et al., 1980; Jackson et al., 1985; Poore et al., 1994). Based on the recently developed age model for Mendeleev Ridge sediments (Kaufman et al., 2008; Adler et al., in press), these layers correspond to age levels near the boundaries between MIS 5/6 and 7/8 (that is, around 130 and 250 ka). The level at which detrital carbonates disappear in all cores, and Ca contents drop to very low values, has been identified in earlier works at the bottom of Clark's unit F (Darby, 1971; Clark et al., 1980). By extrapolating the above ages, this level can be crudely dated to between 300 and 350 ka; a somewhat larger age can be expected in view of the decrease in sedimentation rates below MIS 6 identified on the central Lomonosov Ridge (O'Regan et al., 2008). An additional, older stratigraphic marker is the top of predominantly brown sediment (purple correlation line in Fig. 4b), recovered between 8 and 10 m in cores on the southern Mendeleev Ridge (HLY0503-6 to 8), between 4 and 6 m in the interior of the western Arctic Ocean (e.g., HLY0503-10 to 14), and at less than 3 m in CESAR cores (units A1–A3;

¹ Sediment accumulation rates were not calculated because not all cores had sediment density data.

Jackson et al., 1985). Along the same lines as above, the age of this boundary can be estimated as older than 500 ka, which is generally consistent with the finding of Pliocene foraminifers in the bottom part of core 93AR-23 (Mullen and McNeil, 1995).

The general pattern characterizing both the Northwind and Mendeleev ridge stratigraphies is the overall decrease in the thickness of sedimentary units and, thus, in sedimentation rates from south to north, or away from the continental margin (Fig. 4; see also Phillips and Grantz, 2001). One exception is the expanded stratigraphy in HLY0503-8JPC in comparison with the nearby NP26 cores from shallower water depths (Adler et al., in press) and even with more southerly box core P1-AR94-B8. This variance can be explained by the position of HLY0503-8JPC at the foot of the ridge slope rather than on the crest, leeward of the subsurface currents, which is beneficial for deposition of fine sediment load (Hunkins et al., 1969).

5. Discussion

The developed correlations across the western Arctic Ocean allow for a better understanding of the distribution of sedimentary facies and sedimentation rates, and, thus, transportation and depositional mechanisms. An important aspect that needs to be taken into account in paleoceanographic investigations is the uneven distribution of sedimentation rates both geographically and stratigraphically. The correlation from the Alaskan margin to the southern part of the Northwind Ridge demonstrates a five- to ten-fold decrease in sedimentation rates (ten-fold if Holocene is included), from tens of centimeters to a few centimeters per kyr (Fig. 2). Further decrease continues towards the Mendeleev Ridge and along both ridges northwards, or away from the continental margin (Figs. 2 and 4). These changes are unevenly distributed between various sedimentary units, but the overall trend of basinwards-decreasing sedimentation rates is similar in all units (Fig. 2).

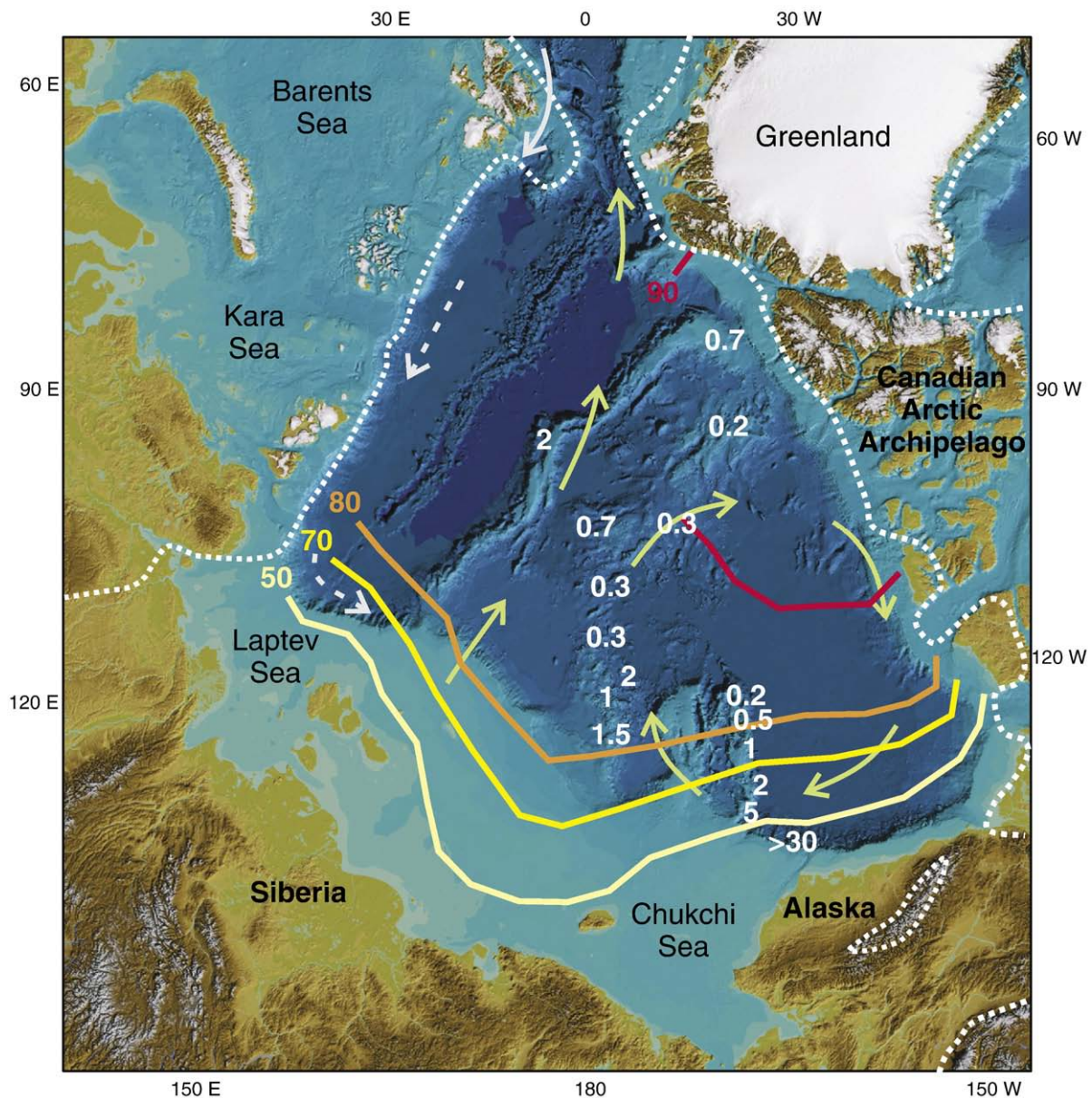


Fig. 5. Average Late Quaternary sedimentation rates in cm/kyr at investigated sites (including published data from 96/12-1PC/ACEX, GreenICE, CESAR, NP26, P1-AR94-B8, and PS-51038-4) and summer sea-ice concentration contours for the late 20th century (in %, from Deser and Teng, 2008; no data near the North Pole). Arrows show major surface circulation features as in Fig. 1. Also shown are the maximal limits of Late Pleistocene glaciations (dotted lines). See Fig. 1 for core numbers and physiographic names.

Average Late Quaternary sedimentation rates estimated in cores based on ^{14}C /AAR ages and the position of major stratigraphic markers (Figs. 2 and 4) are mapped along with multi-year mean contours of modern sea-ice concentration (Fig. 5). To expand the geographic coverage, we add stratigraphic estimates for published sedimentary records from the central Lomonosov Ridge (Jakobsson et al., 2000; O'Regan et al., 2008), the area north of Greenland (GreenICE: Nørgaard-Pedersen et al., 2007), central Alpha Ridge (PS-51038-4: Spielhagen et al., 2004), and Alpha Ridge off the Canadian Archipelago (CESAR: Jackson et al., 1985); for the latter source, we revise the age model based on correlation with HOTRAX cores along the same lines as on Fig. 4. The resulting geographic pattern suggests that long-term, Late Quaternary sedimentation in the western Arctic Ocean is controlled by the combination of sea-ice concentration, and thus melt-out rates, and transportation distance from sediment sources at the continental margins, where the current system is considered. More detailed geographic coverage, especially near the margins is needed to distinguish between these controls. The lowest sedimentation rates of just a few millimeters per kyr occur on the ridges in the interior of the Amerasia Basin, which combines the highest ice concentration with the long transportation pathway in the Beaufort Gyre circulation system. In addition to this general sedimentation pattern, local heterogeneity is possible due to subsurface currents that may cause non-deposition on the ridge crests and deposition in adjacent basins as presumably exemplified by the enhanced sedimentation in HLY0503-8JPC in comparison with nearby cores from the Mendeleev Ridge crest such as NP-26 (Fig. 1) (Adler et al., *in press*); similar depth-dependent variability in sedimentation rates is evident in cores from the central Lomonosov Ridge (O'Regan et al., 2008). Subsurface circulation is also important in affecting the iceberg melt rate, so that periods with reduced inflow of intermediate, warm Atlantic water to the western Arctic during glaciations were likely characterized with less sedimentation from icebergs.

More detailed depositional patterns can be discerned when different sedimentary units are considered. The Holocene, which represents interglacial conditions, is characterized by a sharp gradient in sedimentation rate decrease from the Alaskan margin to the basin interior, between two to three orders of magnitude. This pattern is probably controlled by sea-ice melt-out, with much higher deposition in the ice marginal zone in comparison with perennial ice in the central Arctic, as well as by the modern-type current system at the margin and location of sediment sources (such as river mouths and eroding coasts). We note that sediments are very heterogeneously distributed on the Chukchi Sea floor due to currents that may reach up to 100 cm/s and the uneven seafloor morphology with numerous canyons on the slope (Phillips et al., 1988; Darby et al., *in press*). Glacial/deglacial environments show a somewhat more gradual decrease in sedimentation rates from the Alaskan margin to the Northwind and then Mendeleev Ridge than the Holocene (Fig. 2). This sedimentation regime was dominated by iceberg rafting in the Beaufort Gyre type circulation throughout the western Arctic as demonstrated by high amounts of IRD including detrital carbonates from Canadian sources. This IRD provenance extends to the area north of Greenland on the way to the Fram Strait, but does not cross the central Lomonosov Ridge that was affected by the Transpolar Drift type circulation carrying Eurasian material (Vogt, 1997; Phillips and Grantz, 2001). This circulation, probably combined with a stronger melting effect of Atlantic waters, resulted in relatively elevated sedimentation rates of 1–3 cm/kyr on the central Lomonosov Ridge (Fig. 5) (Backman et al., 2004; O'Regan et al., 2008). Some intervals in Mendeleev Ridge cores, such as the penultimate glaciation that is constrained to ca. 45–55 ka in northern Eurasia (Svendsen et al., 2004; Larsen et al., 2006), contain IRD of inferred Eurasian origin indicating potential swings in circulation or additional glacial sources such as a hypothetical ice sheet on the eastern Siberian shelf (Grosswald, 1980; Tumskey and Basilyan, 2007).

The interval immediately prior to and after the LGM in the western Arctic, roughly corresponding to MIS 2, is characterized by a unique IRD composition predominated by sedimentary clasts, mostly dark-gray siltstones and shales, as well as coal (Fig. 2) (see also Polyak et al., 2007). Rocks of this composition occur at the North American margin, notably in the Mackenzie area and in the north-central part of the Canadian Archipelago (e.g., Dixon et al., 1992; Darby and Bischof, 1996; Phillips and Grantz, 2001), but normally do not make any considerable contribution to IRD in the basin. We infer that these source rocks were subjected to glacial erosion when the northwestern Laurentide limit expanded to the continental margin at low sea level such as during MIS 2. In contrast, peaks of carbonate-composed IRD primarily originate from the more internal areas of the Canadian Arctic Archipelago and therefore mark episodes of ice-sheet instability, probably more common at higher sea levels. It may be especially important that carbonate beds line the inner reaches of deep troughs east of the Mackenzie area, which were the major outlets for ice streams from the northwestern Laurentide sector (Fig. 1; Stokes et al., 2005; 2006; Kleman and Glasser, 2007).

Interstadials represent a mixture of Holocene-like features, such as high numbers of foraminifers and manganese hydroxides in deep-sea sediments or iron-sulfides on the margins, with frequent IRD pulses characteristic of glacial environments. This pattern makes sense as it indicates a combination of relatively high sea level and relatively open water conditions with considerable ice-sheet masses at the perimeter of the basin, at least in North America.

In the interior of the Amerasia Basin, sedimentary units with abundant coarse IRD typically have sedimentation rates relatively elevated for these sites (Fig. 3), which indicates the primary role of icebergs in long-term sediment delivery to the central Arctic Ocean. However, the highest sedimentation rates, in excess of 10 cm/kyr, found on the southern Mendeleev Ridge are probably related to some other depositional controls as at least one of these events is located in a relatively fine-grained interval with little IRD in the early Holocene, around 8–10 ka. Possible causes could be linked to discharge of proglacial lakes or intensification of coastal erosion during deglaciation and sea-level rise, and/or the proximity of the sea-ice margin during the early Holocene warming (e.g., Fisher et al., 2006). More data are needed to understand the distribution and, consequently, the mechanism of these events.

Glacial maxima, exemplified by the LGM, differ from other sedimentary regimes by very fine-grained sediment rapidly decreasing in thickness from the Alaskan margin to the basin interior and forming a hiatus of several thousand year duration over a large part of the western Arctic Ocean; similar hiatuses may be hidden in sediments of earlier glacial periods. This pattern indicates that sedimentation was controlled not by floating ice, be it sea-ice or icebergs, but rather by subsurface lateral water movement. A peculiar composition of this fine sediment such as elevated content of illite and indicators of soil bacteria in biomarkers (Ortiz et al., 2006; Yamamoto and Polyak, *in press*) suggest that it was probably formed by discharge of subglacial erosion into the basin with overflows. One possible mechanism for distribution of this material could be tidal pumping; it has been suggested that tidal forcing was very strong in the glacial Arctic Ocean, especially near the Laurentide ice-sheet margin (Griffiths and Peltier, 2008).

We infer that a regime when water movement instead of floating ice primarily controlled sedimentation in the central Arctic Ocean was possible due to a very solid ice cover with diminutive melt-out over a large part of the basin. Potential causes for this ice conditions may include such exotic scenarios as anomalously thickened sea ice, to tens or even hundreds of meters under very cold air and water temperatures (Grosswald and Hughes, 1999; Bradley and England, 2008), or the extension of large ice shelves from the ice-sheet margins (Polyak et al., 2001; Jakobsson et al., 2008b); evaluation of these hypotheses requires paleoclimatic and paleoglaciological modeling. A more

conservative interpretation implies that the western Arctic had a very high concentration of sea ice during glacial maxima due to a combination of climatic and hydrographic factors such as low temperatures, high amount of meltwater, and sluggish circulation, as well as perennial snow cover that prevented light penetration causing essentially abiotic conditions. This high ice concentration would be similar or even higher than near the eastern part of the Canadian Arctic today, where long-term Quaternary sedimentation rates are as low as 2 mm/kyr (Fig. 5) and were likely even lower during glacial maxima. Under such conditions, the LGM throughout the Amerasia Basin would be represented by just a few millimeters of sediment without datable material because of completely, or almost completely suppressed biological production, which is sufficient to explain the observed age-depth distribution (Fig. 3). This interpretation is consistent with sedimentation patterns from the Eurasia Basin, where the LGM sediment fluxes are somewhat higher, but still very low all the way to about 85° N (Nørgaard-Pedersen et al., 1998, 2003), whereas cores from the Fram Strait demonstrate an increase in deposition during the LGM including numerous IRD with North American sources (Darby et al., 2002; Darby and Zimmerman, 2008). We propose that this pattern depicts the negligible release of sediment from floating ice over the western and sizeable part of eastern Arctic Ocean and the consequent enhanced IRD melt-out and deposition in the Fram Strait. A better geographic coverage combined with adequate age control is needed to reconstruct the LGM paleogeography in the western Arctic.

6. Conclusions

Step-wise correlation of sediment cores from the Alaskan Chukchi margin to the Northwind, Mendeleev, and Alpha ridges, combined with several series of multiple ¹⁴C and/or AAR ages provide stratigraphic background for Late Quaternary paleoceanography in the western Arctic Ocean. The geographic distribution of sediment types and estimated sedimentation rates indicate that the major depositional controls were sea-ice concentration (and thus melt-out rates) and transportation distance from sediment sources at the continental margin. This is reflected in the decrease of average sedimentation rates from tens of centimeters per kyr on the Alaskan margin to a few centimeters at the southern parts of the Northwind and Mendeleev ridges and less than 0.5 cm/kyr in the interior of the Amerasia Basin, consistent with the ice concentration pattern and prevailing Beaufort Gyre circulation system. Subsurface currents may be responsible for some redistribution of sediment such as reduced deposition on ridge crests and enhanced deposition at the lee side of the slopes, as well as for affecting ice melting. Sediment delivery by icebergs, active during glacial periods, appears to have been the overall major contributor of sediment to the deep-sea western Arctic Ocean. On this background, short-term episodes of enhanced sedimentation may have occurred such as in the early Holocene on the southern Mendeleev Ridge; the nature of these sedimentation pulses is yet to be investigated. Iceberg-rafted sediment is mostly related to North American sources, but some glacial intervals may contain Eurasian material as far east as at least the Mendeleev Ridge. Glacial IRD contains pulses of detrital carbonates indicative of the delivery of glacial erosion products from the interior of the Canadian Arctic Archipelago, probably during episodes of ice-sheet instability and activation of ice streams. A different type of IRD composed of sedimentary clasts and coals is presumably related to the erosion of the North American margin during the maximal extension of the Laurentide ice sheet northwestwards at low sea levels such as during MIS 2, immediately prior to and after the LGM.

The interval corresponding to the glacial maximum is composed of distinctly fine-grained sediment that exceeds 2-m thickness on the Alaskan margin and wedges out fast toward the basin interior (Fig. 2). On the Mendeleev Ridge, where sediments have the best age control in the western Arctic Ocean, this interval is almost entirely

represented by a hiatus of several kyr duration, between ca. 15 and 23 ka (maximal age estimate with no ΔR applied; Fig. 3). We relate this sedimentary regime to deposition of fine-grained products of glacial erosion, possibly distributed by tidal currents, under a very concentrated ice cover with perennial snow cover and diminutive melt-out. The broad, pan-Arctic pattern of the LGM sedimentation suggests that this ice covered a large part of the western Arctic Ocean, but was not as extensive in the Eurasia Basin, and co-occurred with enhanced IRD deposition in the Fram Strait that included iceberg-rafted material from North American sources as well as sea-ice IRD from Siberian sources (Darby and Zimmerman, 2008). We infer that similar environments may have existed in the western Arctic during earlier glaciations as well, as suggested by fine-grained intervals in glacial units sharing a common mineralogical composition.

Acknowledgments

Work on this paper was supported by the US NSF-OPP awards ARC-0612473/0612493/0612384 to LP, DD, and JO. We thank the HOTRAX'05 team for help with collection and processing of the HLY0503 cores. R.L. Phillips provided descriptions for P1-92/93-AR cores. M. Torresan helped with additional sampling.

References

- Aagard, K., Barrie, L.A., Carmack, E.C., Garrity, C., Jones, E.P., Lubin, D., Macdonald, R.W., Swift, J.H., Tucker, W.B., Wheeler, P.A., Whritner, R.H., 1996. U.S., Canadian researchers explore Arctic Ocean. *Eos Trans. AGU* 77, 209–213.
- Adler, R.E., Polyak, L., Ortiz, J.D., Kaufman, D.S., Channell, J.E.T., Xuan, C., Grottole, A.G., Sellén, E., Crawford, K.A., in press. Sediment record from the western Arctic Ocean with an improved Late Quaternary age resolution: HOTRAX core HLY0503-8JPC, Mendeleev Ridge. *Global Planet. Change*.
- Andrews, J.T., Dunhill, G., 2004. Early to mid-Holocene Atlantic water influx and deglacial meltwater events, Beaufort Sea slope. *Arctic Ocean. Quat. Res.* 61, 14–21.
- Backman, J., Jakobsson, M., Løvlie, R., Polyak, L., Febo, L.A., 2004. Is the central Arctic Ocean a sediment starved basin? *Quat. Sci. Rev.* 23, 1435–1454.
- Barletta, F., St-Onge, G., Channell, J.E.T., Polyak, L., Darby, D.A., 2008. High-resolution paleomagnetic secular variation and relative paleointensity records from the western Canadian Arctic: implication for Holocene stratigraphy and geomagnetic field behaviour. *Can. J. Earth Sci.* 45, 1265–1281.
- Belov, N.A., Lapina, N.N., 1961. Donnye otlozheniya Arkticheskogo bassejna [Seafloor sediments of the Arctic Basin]. *Morskoy Transport, Leningrad*. 150 p. (in Russian).
- Belov, N.A., Lapina, N.N., 1970. Fluctuations in Arctic climate as revealed in floor sediment analysis. In: Tolmachev, A.I. (Ed.), *The Arctic Ocean and its coasts in the Cenozoic Era*. *Gidrometeorologicheskoe Publishers, Leningrad*, pp. 19–25 (Translated from Russian).
- Bischof, J., Clark, D., Vincent, J., 1996. Pleistocene paleoceanography of the central Arctic Ocean: the sources of ice rafted debris and the compressed sedimentary record. *Paleoceanography* 11, 743–756.
- Bradley, R.S., England, J.H., 2008. The Younger Dryas and the sea of ancient ice. *Quat. Res.* 70, 1–10.
- Clark, D.L., 1970. Magnetic reversals and sedimentation rates in the Arctic Ocean. *GSA Bull.* 81, 3129–3134.
- Clark, D.L., Whitman, R.R., Morgan, K.A., Mackey, S.D., 1980. Stratigraphy and glacial marine sediments of the Amerasian Basin, central Arctic Ocean. *Geol. Soc. Am. Sp. Paper* 181, 57.
- Comiso, J.C., Parkinson, C.L., Gersten, R., Stock, L., 2008. Accelerated decline in the Arctic sea ice cover. *Geophys. Res. Lett.* 35, L01703.
- Darby, D.A., 1971. Carbonate cycles and clay mineralogy of Arctic Ocean sediment cores. Ph.D. Thesis, Univ. Wisconsin-Madison, 43 p.
- Darby, D.A., 2003. Sources of sediment found in sea ice from the western Arctic Ocean, new insights into processes of entrainment and drift patterns. *J. Geophys. Res.*, 108 (C8), 3257.
- Darby, D.A., Bischof, J.F., 1996. A statistical approach to source determination of lithic and Fe-oxide grains: an example from the Alpha Ridge, Arctic Ocean. *J. Sediment. Res.* 66, 599–607.
- Darby, D.A., Zimmerman, P., 2008. Ice-rafted detritus events in the Arctic during the last glacial interval and the timing of the Innuitian and Laurentide ice sheet calving events. *Polar Res.* 27, 114–127.
- Darby, D.A., Bischof, J.F., Jones, G.A., 1997. Radiocarbon chronology of depositional regimes in the western Arctic Ocean. *Deep-Sea Res.* 44, 1745–1757.
- Darby, D.A., Bischof, J., Cutter, G., de Vernal, A., Hillaire-Marcel, C., Dwyer, G., McManus, Osterman, L.J., Polyak, L., Poore, R., 2001. New record of pronounced changes in Arctic Ocean circulation and climate. *Eos Trans. AGU* 82, 603–607.
- Darby, D.A., Bischof, J.F., Spielhagen, R.F., Marshal, S.A., Herman, S.W., 2002. Arctic ice export events and their potential impact on global climate during the late Pleistocene. *Paleoceanography* 15–1 to 15–17.
- Darby, D., Jakobsson, M., Polyak, L., 2005. Icebreaker expedition collects key Arctic seafloor and ice data. *Eos Trans. AGU* 86, 549–556.

- Darby, D.A., Ortiz, J.D., Polyak, L., Lund, S., Jakobsson, M., Woodgate, R.A., in press. The role of currents and sea ice in both slowly deposited central Arctic and rapidly deposited Chukchi-Alaskan margin sediments. *Global Planet. Change*.
- Deser, C., Teng, H., 2008. Evolution of Arctic sea ice concentration trends and the role of atmospheric circulation forcing, 1979–2007. *Geophys. Res. Lett.* 35, L02504.
- De Vernal, A., Hillaire-Marcel, C., Darby, D.A., 2005. Variability of sea ice cover in the Chukchi Sea (western Arctic Ocean) during the Holocene. *Paleoceanography* 20, PA4018.
- Dixon, J., Dietrich, J.R., McNeil, D.H., 1992. Upper Cretaceous to Pleistocene sequence stratigraphy of the Beaufort–Mackenzie and Banks Island areas, northwest Canada. *Bull.—Geol. Surv. Can.* 407 90 p.
- Dyke, A.S., Andrews, J.T., Clark, P.U., England, J.H., Miller, G.H., Shaw, J., Veillette, J.J., 2002. The Laurentide and Innuitian ice sheets during the Last Glacial maximum. *Quat. Sci. Rev.* 21, 9–31.
- Eberl, D.D., 2003. User guide to RockJock: a program for determining quantitative mineralogy from X-ray diffraction data. U.S. Geological Survey, Open File Report, vol. 03–78. 40 p.
- Eberl, D.D., 2004. Quantitative mineralogy of the Yukon River system: variations with reach and season, and determining sediment provenance. *Am. Mineral.* 89, 1784–1794.
- Ekwrzel, B., Schlosser, P., Mortlock, R.A., Fairbanks, R.G., Swift, J.H., 2001. River runoff, sea ice meltwater and Pacific water distribution and mean residence times in the Arctic Ocean. *J. Geophys. Res.* 106, 9075–9092.
- Ericson, D.B., Ewing, M., Wollin, G., 1964. Sediment cores from the arctic and subarctic seas. *Science* 144 (3623), 1183–1192.
- Fairbanks, R.G., Mortlock, R.A., Chiu, T.-C., Cao, L., Kaplan, A., Guilderson, T.P., Fairbanks, T.W., Bloom, A.L., 2005. Marine radiocarbon calibration curve spanning 0 to 50,000 years B.P. based on paired $^{230}\text{Th}/^{234}\text{U}/^{238}\text{U}$ and ^{14}C dates on pristine corals. *Quat. Sci. Rev.* 24, 1781–1796.
- Fisher, D., Dyke, A., Koerner, R., Bourgeois, J., Kinnard, C., Zdanowicz, C., de Vernal, A., Hillaire-Marcel, C., Savelle, J., Rochon, A., 2006. Natural variability of Arctic sea ice over the Holocene. *Eos Trans. AGU* 87, 273–275.
- Griffiths, S.D., Peltier, W.R., 2008. Mega-tides in the Arctic Ocean under glacial conditions. *Geophys. Res. Lett.* 35, L08605.
- Grosswald, M.G., 1980. Late Weichselian ice sheets of northern Eurasia. *Quat. Res.* 13, 1–32.
- Grosswald, M.G., Hughes, T.J., 1999. The case for an ice shelf in the Pleistocene Arctic Ocean. *Polar Geography* 23, 23–54.
- Grygar, T., Polyak, L., Schneeweiss, O., 2007. Nature of Fe-precipitates in sediments from the Mendeleev Ridge, Arctic Ocean. *Geophys. Res. Abstr.* 9, 02001 (European Geosci. Union).
- Heier-Nielsen, S., Heinemeier, J., Nielsen, H.L., Rud, N., 1995. Recent reservoir ages for Danish fjords and marine waters. *Radiocarbon* 37, 875–882.
- Herman, Y., 1969. Arctic Ocean Quaternary microfauna and its relation to paleoclimatology. *Palaeogeogr. Palaeogeoclimatol. Palaeoecol.* 6, 251–276.
- Herman, Y., 1974. Arctic Ocean sediments, microfauna, and the climatic record in late Cenozoic time. In: Herman, Y. (Ed.), *Marine Geology and Oceanography of the Arctic Seas*. Springer-Verlag, Berlin, pp. 283–348.
- Hunkins, K., Thorndike, E.M., Mathieu, G., 1969. Nepheloid layers and bottom currents in the Arctic Ocean. *J. Geophys. Res.* 74, 6995–7008.
- Hunkins, K.L., Be, A.W.H., Opdyke, N.D., Mathieu, G., 1971. The late Cenozoic history of the Arctic Ocean. In: Turekian, K.K. (Ed.), *The Late Cenozoic Glacial Ages*. Yale Univ. Press, pp. 215–237.
- Hwang, J., Eglinton, T.I., Krishfield, R.A., Manganini, S.J., Honjo, S., 2008. Lateral organic carbon supply to the deep Canada Basin. *Geophys. Res. Lett.* 35, L11607.
- Jackson, H.R., Mudie, P.J., Blasco, S.M. (Eds.), 1985. Initial geological report on CESAR—the Canadian expedition to study the Alpha Ridge, Arctic Ocean. *Geol. Survey Canada Paper*, vol. 84–22. 177 p.
- Jakobsson, M., Løvlie, R., Al-Hanbali, H., Arnold, E., Backman, J., Mörth, M., 2000. Manganese color cycles in Arctic Ocean sediments constrain Pleistocene chronology. *Geology* 28, 23–26.
- Jakobsson, M., Lølie, R., Arnold, E., Backman, J., Polyak, L., Knutsen, J., Musatov, E., 2001. Pleistocene stratigraphy and paleoenvironmental variation from Lomonosov Ridge sediments, central Arctic Ocean. *Glob. Planet. Change* 31, 1–21.
- Jakobsson, M., Macnab, R., Mayer, L., Anderson, R., Edwards, M., Hatzky, J., Schenke, H.W., Johnson, P., 2008a. An improved bathymetric portrayal of the Arctic Ocean: implications for ocean modeling and geological, geophysical and oceanographic analyses. *Geophys. Res. Lett.* 35, L07602.
- Jakobsson, M., Polyak, L., Edwards, M.H., Kleman, J., Coakley, B.J., 2008b. Glacial geomorphology of the central Arctic Ocean: Chukchi Borderland and the Lomonosov Ridge. *Earth Surf. Process. Landf.* 33, 526–545.
- Kaufman, D., Polyak, L., Adler, R., Channell, J.E.T., Xuan, C., 2008. Dating late Quaternary planktonic foraminifer *Neogloboquadrina pachyderma* from the Arctic Ocean by using amino acid racemization. *Paleoceanography* 23, PA3224.
- Keigwin, L.D., Donnelly, J.P., Cook, M.S., Driscoll, N.W., Brigham-Grette, J., 2006. Rapid sea-level rise and Holocene climate in the Chukchi Sea. *Geology* 34, 861–864.
- Kirschvink, J.L., 1980. The least squares lines and plane analysis of paleomagnetic data. *Geophys. J.R. Astr. Soc.* 62, 699–718.
- Kleman, J., Glasser, N.F., 2007. The subglacial thermal organisation (STO) of ice sheets. *Quat. Sci. Rev.* 26, 585–597.
- Larsen, E., Kjær, K.H., Demidov, I.N., Funder, S., Grøsfjeld, K., Houmark-Nielsen, M., Jensen, M., Linge, H., Lysa, A., 2006. Late Pleistocene glacial and lake history of northwestern Russia. *Boreas* 35, 394–424.
- Lisé-Pronovost, A., St-Onge, G., Brachfeld, S., Barletta, F., Darby, D.A., in press. Paleomagnetic constraints on the Holocene stratigraphy of the Arctic Alaskan margin. *Global Planet. Change*.
- Löwemark, L., Jakobsson, M., Mörth, M., Backman, J., 2008. Arctic Ocean Mn contents and sediment colour cycles. *Polar Res.* 27, 105–113.
- Mangerud, J., Gulliksen, S., 1975. Apparent radiocarbon ages of recent marine shells from Norway, Spitsbergen, and Arctic Canada. *Quat. Res.* 5, 263–273.
- McKay, J.L., de Vernal, A., Hillaire-Marcel, C., Not, C., Polyak, L., Darby, D.A., 2008. Holocene fluctuations in Arctic sea-ice cover: dinocyst-based reconstructions for the eastern Chukchi Sea. *Can. J. Earth Sci.* 45, 1377–1397.
- McNeely, R., Dyke, A.S., Southon, J.R., 2006. Canadian marine reservoir ages, preliminary data assessment, Open File 5049. *Geol. Survey of Canada*, p. 3.
- Mullen, M.W., McNeil, D.H., 1995. Biostratigraphic and paleoclimatic significance of a new Pliocene foraminiferal fauna from the central Arctic Ocean. *Mar. Micropaleontol.* 26, 273–280.
- Nørgaard-Pedersen, N., Spielhagen, R., Thiede, J., Kassens, H., 1998. Central Arctic surface ocean environment during the past 80,000 years. *Paleoceanography* 13, 193–204.
- Nørgaard-Pedersen, N., Spielhagen, R.F., Erlenkeuser, H., Grootes, P.M., Heinemeier, J., Knies, J., 2003. Arctic Ocean during the Last Glacial Maximum: Atlantic and polar domains of surface water mass distribution and ice cover. *Paleoceanography* 18, 1063.
- Nørgaard-Pedersen, N., Mikkelsen, N., Kristoffersen, Y., 2007. Arctic Ocean record of last two glacial–interglacial cycles off North Greenland/Ellesmere Island—implications for glacial history. *Mar. Geol.* 244, 93–108.
- O'Regan, M., King, J., Backman, J., Jakobsson, M., Pälike, H., Moran, K., Heil, C., Sakamoto, T., Cronin, M., Jordan, R., 2008. Constraints on the Pleistocene chronology of sediments from the Lomonosov Ridge. *Paleoceanography* 23, PA1519.
- Ortiz, J.D., Polyak, L., Jakobsson, M., Darby, D., 2006. Quaternary inferences on central Arctic Ocean circulation and sediment provenance based on Diffuse Spectral Reflectance analysis. *Eos Trans. AGU* 87 (52) Fall Meet. Suppl., Abstract OS53B-1098.
- Ortiz, J.D., Polyak, L., Grebmeier, J.M., Darby, D.A., Eberl, D.D., Naidu, S., Nof, D., in press. Provenance of Holocene sediment on the Chukchi-Alaskan margin based on combined diffuse spectral reflectance and quantitative X-Ray Diffraction analysis. *Global Planet. Change*.
- Phillips, R.L., Grantz, A., 1997. Quaternary history of sea ice and paleoclimate in the Amerasia basin, Arctic Ocean, as recorded in the cyclical strata of Northwind Ridge. *Geol. Soc. Am. Bull.* 109, 1101–1115.
- Phillips, R.L., Grantz, A., 2001. Regional variations in provenance and abundance of ice-rafted clasts in Arctic Ocean sediments: implications for the configuration of late Quaternary oceanic and atmospheric circulation in the Arctic. *Mar. Geol.* 172, 91–115.
- Phillips, R.L., Barnes, P., Hunter, R.E., Reiss, T.E., Rearic, D.M., 1988. Geologic investigation in the Chukchi Sea, 1984, NOAA ship SURVEYOR cruise. USGS Open-file Report, vol. 88–25. 82 p.
- Polyak, L., Edwards, M.H., Coakley, B.J., Jakobsson, M., 2001. Ice shelves in the Pleistocene Arctic Ocean inferred from glaciogenic deep-sea bedforms. *Nature* 410 (6827), 453–459.
- Polyak, L., Curry, W.B., Darby, D.A., Bischof, J., Cronin, T.M., 2004. Contrasting glacial/interglacial regimes in the western Arctic Ocean as exemplified by a sedimentary record from the Mendeleev Ridge. *Palaeogeogr. Palaeoclimatol.* 203, 73–93.
- Polyak, L., Darby, D.A., Bischof, J., Jakobsson, M., 2007. Stratigraphic constraints on late Pleistocene glacial erosion and deglaciation of the Chukchi margin, Arctic Ocean. *Quat. Res.* 67, 234–245.
- Poore, R., Phillips, L., Rieck, H., 1993. Paleoclimate record for Northwind Ridge, western Arctic Ocean. *Paleoceanography* 8, 149–159.
- Poore, R., Ishman, S., Phillips, L., McNeil, D., 1994. Quaternary stratigraphy and paleoceanography of the Canada Basin, western Arctic Ocean. *US Geol. Surv. Bull.* 2080, 32.
- Poore, R.Z., Ostermann, D.R., McGeehin, J., 1999a. Stable isotope data and AMS ^{14}C dates from Arctic Ocean Section 1994 surface sediment transect and box core samples from the Mendeleev Ridge area USGS Open-File Report. USGS Open-File Report vol. 99–48, 17.
- Poore, R., Ostermann, L., Curry, W., Phillips, R., 1999b. Late Pleistocene and Holocene meltwater events in the western Arctic Ocean. *Geology* 27, 759–762.
- Scientific Party, 1993. Cruise to the Chukchi Borderland, Arctic Ocean. *Eos Trans. AGU* 74, 253–254.
- Sellén, E., Jakobsson, M., Backman, J., 2008. Sedimentary regimes in Arctic's Amerasian and Eurasian basins: clues to differences in sedimentation rates. *Global Planet. Change* 61, 275–284.
- Spielhagen, R., Baumann, K., Erlenkeuser, H., Nowaczyk, N., Nørgaard-Pedersen, N., Vogt, C., Weiel, D., 2004. Arctic Ocean deep-sea record of northern Eurasian ice sheet history. *Quat. Sci. Rev.* 23, 1455–1483.
- Stein, R., Schubert, C., MacDonald, R.W., Fahl, K., Harvey, H.R., Weiel, D., 2004. The central Arctic Ocean: distribution, sources, variability and burial of organic carbon. In: Stein, R., MacDonald, R.W. (Eds.), *The Organic Carbon Cycle in the Arctic Ocean*. Springer, Berlin, pp. 295–314.
- Steuerwald, B.A., Clark, D.L., Andrew, J.A., 1968. Magnetic stratigraphy and faunal patterns in Arctic Ocean sediments. *Earth Planet. Sci. Lett.* 5, 79–85.
- Stokes, C., Clark, C., Darby, D., Hodgson, D., 2005. Late Pleistocene ice export events into the Arctic Ocean from the McClure Strait Ice Stream, Canadian Arctic Archipelago. *Glob. Planet. Change* 49, 139–162.
- Stokes, C.R., Clark, C.D., Winsborrow, M.C.M., 2006. Subglacial bedform evidence for a major paleo-ice stream and its retreat phases in Amundsen Gulf, Canadian Arctic Archipelago. *J. Quat. Sci.* 21, 399–412.
- Stroeve, J., Serreze, M., Drobot, S., et al., 2008. Arctic sea ice extent plummets in 2007. *Eos Trans. AGU* 89, 13–14.

- Svendsen, J.I., Alexanderson, H., Astakhov, V.I., Demidov, I., Dowdeswell, J.A., Funder, S., Gataullin, V., Henriksena, M., Hjort, C., Houmark-Nielsen, M., Hubberten, H.W., Olfsson, I., Jakobsson, M., Kjæri, K.H., Larsen, E., Lokrantz, H., Pekka Lunkka, J., Lyså, A., Mangeruda, J., Matiouchkov, A., Murray, A., Möller, P., Niessen, F., Nikolskaya, O., Polyak, L., Saarnisto, M., Siegert, M., Spielhagen, R.F., Stein, R., 2004. Late Quaternary ice sheet history of northern Eurasia. *Quat. Sci. Rev.* 23, 1229–1271.
- Syvitski, J.P.M., 1991. Towards an understanding of sediment deposition on glaciated continental shelves. *Cont. Shelf Res.* 11, 821–842.
- Tumskoy, V. and Basilyan, A., 2007. Geological, permafrost and glacial interactions in Siberian Arctic: an idea for an new international project, First Conference on Arctic Palaeoclimate and its Extremes: Planning of International Polar Year Activities and Preliminary Results. Stockholm University, Royal Swedish Academy of Sciences, Stockholm, Sweden.
- Vogt, C., 1997. Regional and temporal variations of mineral assemblages in Arctic Ocean sediments as climatic indicator during glacial/interglacial changes. *Reports Polar Res.* 251 309 p. (in German).
- Yamamoto, M., Polyak, L., in press. Changes in terrestrial organic matter input to the Mendeleev Ridge, western Arctic Ocean, during the Late Quaternary. *Global Planet. Change*.